How to Cite:
Ritesh, Chaurasia, H., & Singh, R. (2022). Design, optimization, characterization of dapagliflozin loaded nlc using box-behnken design. *International Journal of Health Sciences*, *6*(S3), 7690–7711. https://doi.org/10.53730/ijhs.v6nS3.7932

Design, optimization, characterization of dapagliflozin loaded nlc using box-behnken design

Ritesh
AdarshVijendra Institute of Pharmaceutical Sciences, Saharanpur, Uttar Pradesh

Himanshu Chaurasia
AdarshVijendra Institute of Pharmaceutical Sciences, Saharanpur, Uttar Pradesh

Ranjit Singh
AdarshVijendra Institute of Pharmaceutical Sciences, Saharanpur, Uttar Pradesh

***Abstract*---**Dapagliflozin used to improve glycemic control, along with diet and exercise, in adults with type 2 diabetes is the model drug selected in the present research titled Design, Optimization, and Characterization of Dapagliflozin Loaded NLC Using Box-Behnken Design. Nano formulations are capable of providing site-specific delivery of anti-diabetic molecules to their specific site of action; this enhances the loco-regional concentration of the drug and reduces the systemic side-effects. Dapagliflozin loaded NLCs were prepared by emulsion–evaporation technique using Stearic acid as lipid and tweens & spans as surfactant. NLCs were characterized for particle size, zeta potential, entrapment efficiency and % drug release. The effects of composition of lipid materials and surfactant mixture and homogenization speed on the particle size, zeta potential, drug entrapment efficiency and in vitro drug release behavior were optimized. The optimized formulation OPT-DP-NLC has shown a particle size, entrapment efficiency and Zeta potential within projected limits, at 69.99 nm, 81.94% and -28.99 respectively.

***Keywords*---**dapagliflozin, NLC, Box-Behnken design, emulsion–evaporation method, hot homogenizaion method, particle sizes, entrapment efficiency, DSC, TEM.

Introduction

Nanotechnology is a leading scientific technique that offers sensing technologies and miniature devices to diagnose disease accurately and within time. Nano formulations are also capable of providing site-specific delivery of anti-diabetic

molecules to their specific site of action; this enhances the loco-regional concentration of the drug and reduces the systemic side-effects (Gadadare et al., 2015). (P-gp) pump or via targeting specific receptors which further improve the pharmacokinetic Most importantly, nano formulations also act at molecular level to enhance the cellular drug uptake or block efflux mechanisms like P-glycoprotein and pharmacodynamic profile of anti-diabetic molecules. Thus, considering these advantages of nanoformulations, the present work was designed to focus on different types of nanoformulations of anti-diabetic drug. A number of lipid based nanosystems (Figure 1) including SEDDS, SLNs, NLCs and vesicular delivery systems have been studied to deliver drugs via transdermal route. Sustained hypoglycemic effect and improved transdermal flux are some of the advantages offered by incorporating nano formulations in TDP. (Veiseh et al., 2015).

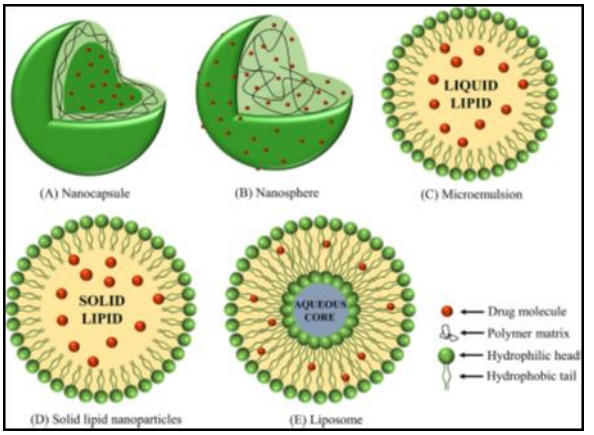

Fig. 1. Types of Lipid-based Nanoparticles

Diabetes

Diabetes mellitus, often simply referred to as diabetes is a group of metabolic diseases in which a person has high blood sugar, either because the body does not produce enough insulin, or because cells do not respond to the insulin that is produced. This high blood sugar produces the classical symptoms of polyuria (frequent urination), polydipsia (increased thirst) and polyphagia (increased hunger) (Matthaei et al., 2000). So aim of present work was to Develop Characterize and optimize Anti-diabetic drug loaded nanoparticle formulation with enhanced oral bioavailability. Dapagliflozin was the model drug selected for the current work. Dapagliflozin is a C-glycosyl comprising beta-D-glucose in which the anomeric hydroxy group is replaced by a 4-chloro-3-(4-ethoxybenzyl) phenyl group. Used (in the form of its propanediol monohydrate) to improve glycemic control, along with diet and drug excercise, in adults with type 2 diabetes.

Material and Methods

Dapagliflozin purchased from Sisco RL Pvt Ltd. Mumbai, surfactants like Tweens (20, 40, 60, 80 grades), spans (20, 40, 60, 80 grades), other solvents like Stearic

Acid, and Dichloromethane are procured from SD Fine Chemicals Mumbai.

Experimental design, method of preparation

Box-Behnken Experimental Design (Aslam et al., 2015)

Box-Behnken statistical design (BBD) with 3 factors (Lipid concentration; X1, surfactant amount; X2, and RPM; X3), and with 3levels (−1, 0, and 1) (Table 1&2) was built up to estimate the significance effect of these different variables on the responses namely, VZ, DEE and % drug release, and then predicts the optimized NLC formulae. BBD is appropriate to explore quadratic response surfaces and assemble second-order polynomial equations. The polynomial equation (Eq. (1)) was derived using a Design Expert software program (Version 12 Stat-Ease Inc., Minneapolis, MN). The dependent and independent variables are selected after screening of polymer

Formulation of NLCs by solvent evaporation method

The drug loaded NLCs were prepared by solvent evaporation method. Accurately weighed amount of drug (10 mg), and lipid (Steric acid) at different ratios were dissolved in 5 mL chloroform in a 100 mL round bottom flask (RBF). The RBF was attached to the rotavapor (BUCHI, Switzerland) and maintained at 40 °C. Rotation speed of RBF was adjusted to 40 rpm, and vacuum was applied to aid the evaporation of chloroform and to form a thin layer of lipids on the inner wall of the RBF, for 30 min. The vacuum was released, and RBF was kept in a vacuum desiccator for 24 h to completely remove the residual traces of chloroform. Accurately weighed amount of surfactant was dissolved in specified aqueous phase, and 10 mL was added as hydration media into the RBF. The lipid film was removed by hand shaken method in a water bath at 40 °C. A milky white uniform solution was obtained which was further reduced in size by probe sonication (ice bath) at an amplitude of 60%, pulse 2 pulse/sec for specified time. Uniform dispersion of nanoparticles obtained was centrifuged at 4000 rpm for 10 min using a cooling centrifuge at 4 °C to remove microparticles (Alam et al., 2016)

Table 1
Description of Variable

Independent Factor	Level High(+1) Medium(0) Low(-1)			
X1	Sonication Time(s)	-	--	--
X2	Amount of solid lipid(mg)	-	--	--
X3	Surfactant concentration(mg)	-	--	--
Dependent variable(Response)	Particle size(Y1) EE%(Y2) Drug Release(Y3)			

Table 2
Box-Behnken Experimental Design with Coded value

Batch Code	Sonication Time (X_1)	Amount of solid lipid (X_2)	Surfactant (X_3)
DNLC1	+1	+1	0
DNLC2	+1	-1	0
DNLC3	+1	0	0
DNLC4	+1	+1	+1
DNLC5	-1	+1	-1
DNLC5	-1	-1	0
DNLC6	-1	+1	+1
DNLC7	-1	+1	-1
DNLC8	0	-1	0
DNLC9	0	+1	+1
DNLC10	0	+1	-1
DNLC11	0	-1	0
DNLC12	+1	+1	+1
DNLC13	-1	+1	-1
DNLC14	0	-1	0
DNLC15	-1	+1	0

In Vitro Characterization of Drug Loaded NLCs
Determination of Particle Size and Zeta Potential

The hydrodynamic diameter (z-average value) and size distribution of blank NLCs and DRUG-loaded NLCs were analyzed using Malvern Zetasizer (Nano ZS; Malvern Instruments, Malvern, UK) at 25C. (Chen et al., 2014) Zeta potential of DRUG-loaded NLCs was determined by using Malvern Zetasizer on the basis of an electrophoretic light scattering technique (Teixeira et al., 1998). The ZP value reveals the electric charge on the NLC surface and physical stability of these NLCs. The samples were appropriately diluted with milli-Q water to obtain about 100-250 kilo counts per second before analysis. The observations were noted in triplicates (n =3).

Determination of Entrapment Efficiency and Drug-Loading Capacity

The % EE of drug loaded NLCs was determined by the separation of unencapsulated drug from the NLCs by centrifugation at 6000 g at 4C for 20 min. The supernatant containing the unencapsulated DRUG was quantified by the aforementioned HPLC technique. The calculation of EE percentage and the actual and theoretical drug loading capacity were determined by using the following equations:

$$\text{Entrapment Efficiency (\% } w/w) = \frac{(\text{Amount of drug added in NLC} - \text{Amount of free drug})}{(\text{Amount of drug added in NLC})} \times 100$$

$$\text{Actual Drug Loading capacity (mg/g of total lipid)} = \frac{(\text{Amount of drug added in NLC} - \text{Amount of free drug})}{(\text{Amount of total lipid in grams})}$$

$$\text{Theoretical Drug Loading capacity (mg/g of total lipid)} = \frac{(\text{Amount of drug added in NLC})}{(\text{Amount of total lipid in grams})}$$

Surface Morphology (Maringanti et al., 2013)

The morphological characteristic of drug -loaded NLCs was assessed by transmission electron microscopy (TEM; TOPCON002B; Tokyo, Japan) by means of a negative-staining method. For TEM measurement, aqueous dilution of particles was dropped on a 200- mesh copper grid coated with carbon and then stained by adding a drop of 4% (w/v) phosphotungstic acid solution for enhancement of contrast. The surface characteristics of freeze-dried drug-loaded NLCs were visualized by scanning electron microscopy (SEM; Zeiss Gemini 5 1530 FEG).

Differential Scanning Calorimetry

DSC analysis of drug and lyophilized drug-loaded NLCs were carried out using Pyris 6 DSC (Perkin Elmer Software, Pyris series) to analyze the stability and crystallinity of NLCs matrix. The physical states of DRUG and DRUG-loaded NLCs were investigated by powder X-ray diffractometry technique. PXRD of all the samples were performed at 2q from a range of 10C-80C with a Cu Ka radiation source using an Ultima IV X-ray Diffractometer (Rigaku, Tokyo, Japan).

In Vitro Drug Release Study

The drug release study of drug and drug-loaded NLCs was conducted by dialysis bag method. Before the experimentation, the dialysis bag (molecular weight cutoff 10 kDa) was soaked in the dissolution medium overnight. Ten milligrams of sample was dissolved in 5 mL of dissolution media (0.5% v/v Tween 80 in phosphate buffer saline, pH 7.4) and was placed into a dialysis bag with both the ends tightly tied with thread. This bag was immersed into the 50-mL dissolution media and stirred at 100 rpm at 37 ± 0.5C for 24 h. After specific time intervals, 1 mL of the sample was withdrawn through a side tube and immediately replaced with an equal amount of fresh dissolution medium. Then, the samples were filtered by using a 0.45-mm filter and analyzed by aforementioned UV method. Release kinetics modeling was performed by putting the cumulative release data into the zero-order, first-order, HixsonCrowell, Higuchi, and Korsmeyer-Peppas release kinetics models, and the model with the highest value of correlation coefficient (R2) was taken as the best fit model.

Intestinal Permeation Study

Intestinal permeation study was conducted by noneverted gut sac model using female wistar rats weighing 250-300 g. Animal experiments were conducted as per protocol No. 1402 permitted by Institutional Animal Ethical Committee, Jamia Hamdard. Permeation study was conducted with slight modification as reported. (Kasim et al., 2004) Animals were fasted overnight and sacrificed through cervical dislocation under analgesic ethyl ether. The intestine was removed surgically and washed with saline; 5-cm-long ileum was taken by cutting the small intestine. The mucosal side was filled with DRUG suspension (0.25% w/v CMC-Na), and the 2 ends of the intestine were ligated tightly with thread. The sac comprising DRUG suspension was immerged in jacketed glass containing Tyrode's buffer (10 mL), prewarmed to 37 ± 0.5C with consistent stream of hot water in jacket and oxygenated with 95% O2 for 120 min through an aerator. For the quantification of drug transported from mucosal to serosal compartment, 0.5 mLof the sample was taken from the serosal compartment and replenished with equal amount of fresh Tyrode's buffer at specified time intervals. The samples were filtered by means of a membrane filter of 0.45 mm pore size, and the amount of drug permeated through the intestine was measured by the aforementioned UV technique.

Preformulation Studies

Identification of Drug
FTIR Study

The vibrational spectrum of a molecule is a unique physical property of that molecule and can be used as a fingerprint for identification of the compound. The IR spectrum of Dapagliflozin shown in was generated using a Spectrum 100 FT-IR spectrometer (Perkin Elmer®, Beaconsfield, Buckinghamshire, England) from 4000 to 650 cm-1

Solubility

The equilibrium solubility of Dapagliflozin was studied in various solvents. A small excess quantity (approximately 25mg) was taken with 10ml of each investigated solvents in 25ml volumetric flask at room temperature (25°C). Increment of drug was added to each conical flask until undissolved particles were seen even after equilibration for 8 hrs with intermittent shaking. The supernatant liquid was analyzed spectrophotometrically for the drug dissolved until two successive readings of analysis were constant.

Results and Discussion

Pre-formulation studies
FTIR Study

The FTIR study of Dapagliflozin was carried out and spectra obtained is shown in Figure 2 and table 4.

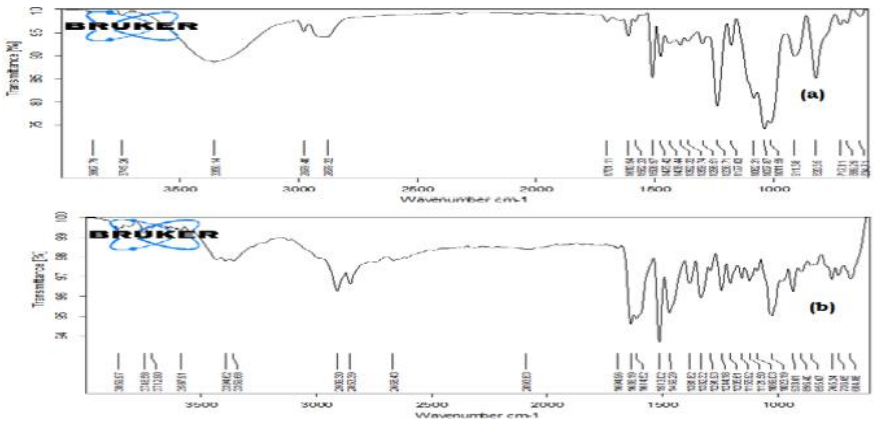

Fig 2. FTIR spectra of Dapagliflozin

Solubility Study of Drugs

Dapagliflozin was found to be insoluble in water and soluble in almost all solvents. Data shown in Figure 3.

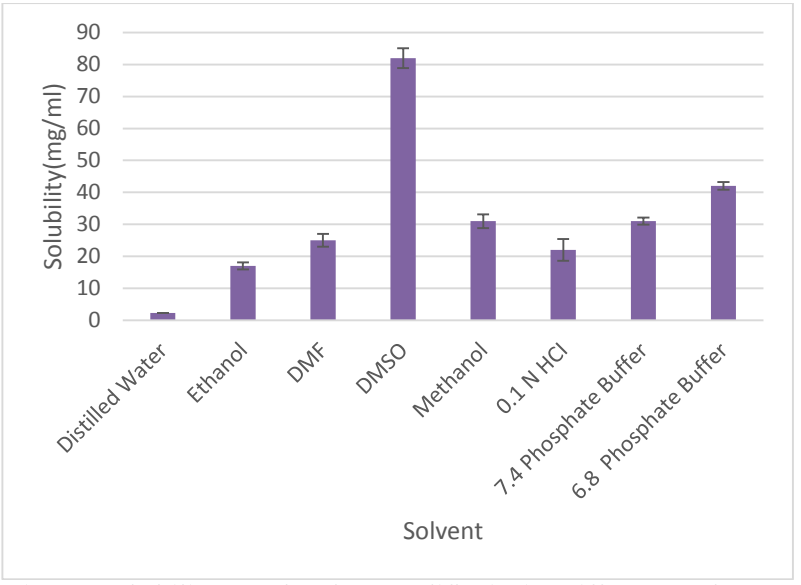

Fig. 3. Solubility Study of Dapagliflozin in Different Solvents

Design, optimization, characterization of dapagliflozin loaded nlc using box-behnken design

Formulation of Dapagliflozin Loaded NLC
Selection of Excipients
Selection of Lipid

The solubility of the drug was determined in different lipids – Glyceryl monostearate, Glyceryl behenate (Compritol 888 ATO), Glyceryl palmitostearate and Cetyl palmitate. The results obtained are as shown below in Table 3 and fig 4.

Table 3
Solubility of Dapagliflozin in different lipids

Lipids	Melting point range ^{0}C	Drug solubility in lipid
Glyceryl monostearate (GMS)	58-59	45±6.04
Compritol 888 ATO (Glyceryl behenate) (CMP)	70-71	110±8.01
Glyceryl palmitostearate (GPS)	53-57	46±5.01
Cetylpalmitate (CP)	43-57	51±5.11

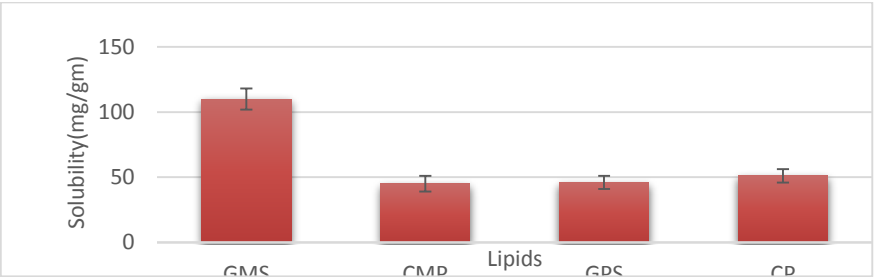

Fig 4. Solubility of Dapagliflozin in different lipids

Selection of Surfactant

For the selection of surfactant, nanoparticles were prepared with six different surfactants using tripalmitin as lipid and were evaluated for particle size and entrapment efficiency. The results obtained are as shown in Table 4 and fig 5.

Table 4
Selection of surfactants by evaluating particle size and entrapment efficiency

S. No.	Lipid	Surfactant	Particle size(nm)	Entrapment Efficiency(%)
1	GMS	Tween 80	252±7.84	51.21±2.84
2	GMS	Tween 20	450±8.04	47.21±1.32
3	GMS	Poloxamer188	332±6.83	40.12±4.21
4	GMS	Tween 60	362±9.01	39.23±4.65
5	GMS	Span 60	512±7.11	30.54±2.35
6	GMS	Span 80	411±8.84	42.87±6.25

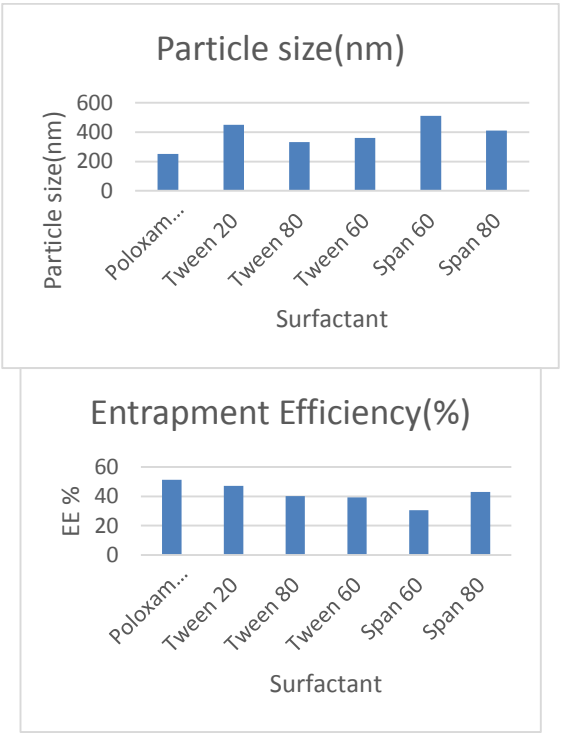

Fig. 5. Particle size and Entrapment efficiency of different surfactants

Differential Scanning Calorimetry (DSC)

Differential Scanning Calorimetry (DSC) excipients were used to find out the presence of any interaction among drug and the excipients and also to find out whether there is any alteration in the crystallinity of the drug. Figure 6 depicts the results obtained by DSC studies.

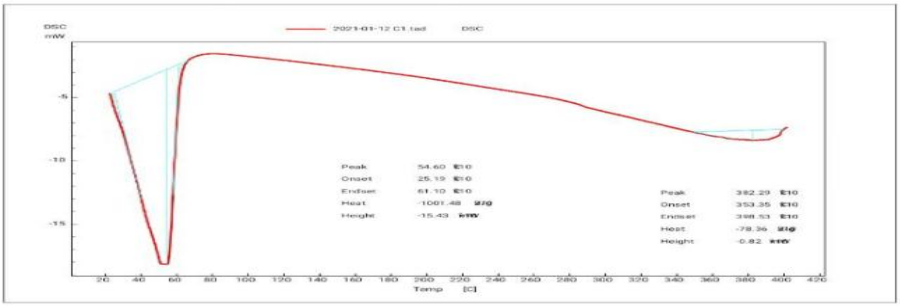

Fig 6. DSC of Pure Dapagliflozin

Formulation tables for Box -Behnken Design with Coded value and Dapagliflozin loaded NLC are tabulated in Table 5.

Table 5
Formulation Table for Dapagliflozin loaded NLC (DPNLC)

Formulation	GMS (mg)X1	Span 80(ml)X2	Co-Surfactant (mg)X3
DPNLC1	100	7.5	20
DPNLC2	50	7.5	20
DPNLC3	50	7.5	10
DPNLC4	75	10	20
DPNLC5	50	10	15
DPNLC6	100	7.5	10
DPNLC7	75	7.5	15
DPNLC8	75	5	10
DPNLC9	100	5	15
DPNLC10	50	5	15
DPNLC11	75	7.5	15
DPNLC12	100	10	15
DPNLC13	75	7.5	15
DPNLC14	75	5	20
DPNLC15	75	10	10

Characterization of Dapagliflozin Loaded NLC (DPNLC)

Characterization of Dapagliflozin loaded NLCs was carried out and the results are tabulated in Table 6

Table 6
Characterization parameters for Dapagliflozin loaded NLCs (DPNLC)

Formulation	Particle Size(nm)	Entrapment Efficiency	Zeta potential(mV)
DPNLC1	112±10.01	90.14±0.01	-21.21
DPNLC2	92±8.02	84.98±0.01	-22.47
DPNLC3	95±11.02	86.59±0.03	-19.74
DPNLC4	82±9.04	92.41±0.01	-22.34
DPNLC5	78±11.01	81.94±0.01	-18.12
DPNLC6	101±11.01	84.36±0.01	-21.12
DPNLC7	85±10.01	84.51±10.01	-23.11
DPNLC8	98±10.02	83.44±10.01	-18.27
DPNLC9	84±9.03	90.11±10.01	-21.14
DPNLC10	65±10.01	92.45±10.01	-19.24
DPNLC11	86±6.11	86.44±10.01	-27.32
DPNLC12	102±11.01	83.14±10.01	-29.24
DPNLC13	84±13.04	91.47±10.01	-21.23
DPNLC14	80±9.01	92.46±10.01	-28.21
DPNLC15	105±11.33	86.21±10.01	-21.31

Particle size were found to be lowest (DPNLC-10) at low levels of the solid lipid, i.e., GMS, high levels of surfactant, i.e., Span 80 and intermediate levels of co-surfactant Drug entrapment values were found to be acceptable around the intermediate levels of lipids and surfactant. This can be ascribed to the presence of sufficient lipids to dissolve the drug and surfactant to emulsify the lipids. The excessively high particle size of DPNLC-1 can be attributed to the presence of high amount of the lipid and intermediate amount of the surfactant to emulsify the lipid completely. Similar results have been obtained in previously reported studies, where low levels of surfactant and high levels of lipid led to the formation of NLCs with high magnitude of particle size and low value of drug entrapment (Bhalekaret al., 2009; Muller et al., 2002; Tran et al., 2014). The lower lipid levels were found to be instrumental in bringing down the particle size of the formulation DPNLC-5 and DPNLC-3. However, the entrapment efficiency of these formulations was found to be acceptable too, probably due to the low levels of the surfactant present in the formulation

Zeta Potential

Figure 7 summarizes the values of zeta potential of all formulations prepared as per the experimental design. The formulations at intermediate levels exhibited high zeta potential, which are further supported by their low particle sizes.

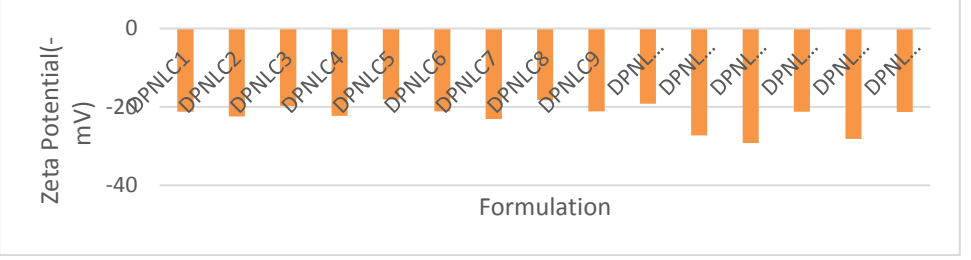

Fig. 7. Zeta potential of Dapagliflozin loaded NLC (DP-NLC)

***In-vitro* Drug Release for DPNLC**

In vitro drug release profile of all developed DG-NLCs and DG-dispersion were carried by using dialysis bag in simulated intestinal fluid as release media (phosphate buffer, pH 6.8. The drug release of all DG-NLCs was found in the range of 63.44 to 83.62**%**(Table 7 and 8). The DG-NLCs-opt exhibited dual release pattern, initial fast release (21.3±3.12**%** in 1 h) followed by slow and prolonged release (90.01±2.01**%**.Initial fast release is due to presence of DG on NLCs surface and slow is due to erosion or degradation of lipid core matrix. The comparative cumulative Dapagliflozin release with respect to time is illustrated in Figure 8. The Dapagliflozin NLC showed biphasic drug release pattern with about 86 % in 8h then about 80-86% of drug was released around 24h.The developed formulation showed initial burst release due to free entrapped drug and/or adsorbed drug to the surface of the nanoparticles. The results also indicate that the drug release from NLC was greatly decreased as the GMS concentration was

increased. The in-vitro release studies reveal that the amount of drug release is increased as the concentration of the span 80 is increase.

Table 7
In-vitro Drug release study (DPNLC1 to DPNLC8)

Tim (hr)	Pur e dru g	DNLC 1	DNLC 2	DNLC 3	DNLC 4	DNLC 5	DNLC 6	DNLC 7	DNLC 8
0	0	0	0	0	0	0	0	0	0
1	30	10	9	8.5	11.3	14.1	11.5	12.6	9.8
2	67.3	20.2	21.4	21.1	22.3	23.1	20.5	24.2	25
4	78.9	33.4	32.1	38.5	34	37.3	36.5	37.8	39.4
6	86.5	45.3	47.8	49.1	50.6	48.7	46.2	49.9	45.4
8	100	61.3	63.8	68.9	70.5	62.4	67.6	68.9	70.2
1 0	100	76.3	78.9	75.6	79.1	74.6	80.6	80.1	79.5
1 2	100	96.8	97.2	96.2	99.1	96.7	96.4	100.2	98.6
2 4	100	99	98.4	97.5	99.4	98.4	100.2	100.1	98.4

Table 8
In-vitro Drug release study (DPNLC8 to DPNLC15)

Time (hr)	DNLC9	DNLC10	DNLC11	DNLC12	DNLC13	DNLC14	DNLC15
0	0	0	0	0	0	0	0
1	8.6	13.4	11.4	14.8	15	12.8	11
2	20.8	22.5	24.6	25.1	21.3	22.4	24.5
4	32.1	35.7	36.8	37.7	38.1	32.5	34.2
6	50.1	47.3	48.6	49.2	50.1	47.3	48.3
8	65.2	66.3	64.8	69.1	62.8	64.9	70.4
10	78.2	76.8	77.8	79.4	80.4	79.4	75.6
12	96.1	98.2	99.1	100.5	97.4	95.7	99.4
24	99.6	99.7	99.1	100.5	98.5	99.4	99.7

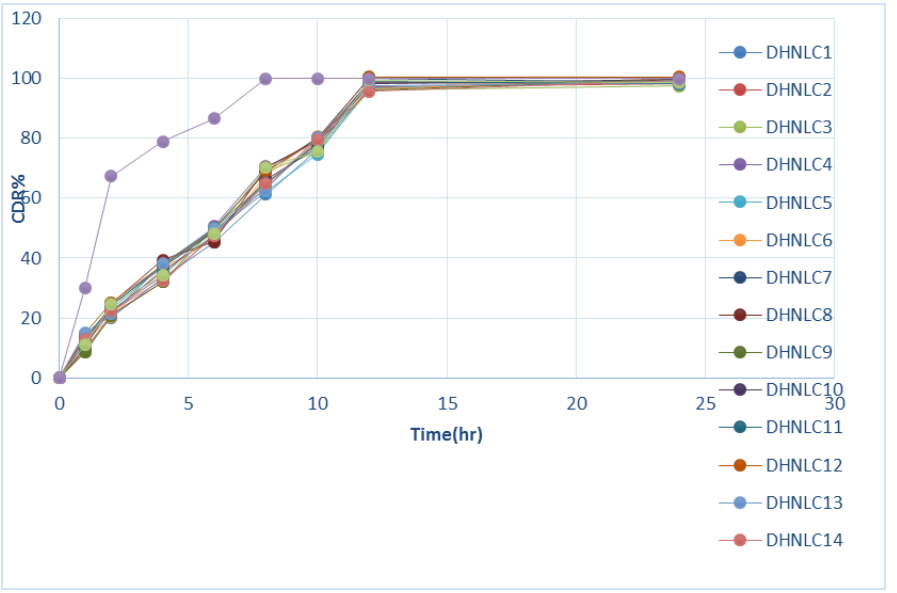

Fig 8. Cumulative Dapagliflozin release with respect to time

Optimization by Box-Behnken Design

ANOVA Table for Particle size, Entrapment Efficiency% and Zeta potential are tabulated in Tables 9-11 respectively. Response Surface Plots showing effect of independent variable on Particle size, Entrapment Efficiency% and Zeta potential are shown in Figures 9-11, respectively.

Table 9
ANOVA Table for Particle size Quadratic model

Response 1: Particle size

Source	Sum of Squares	df	Mean Square	F-value	p-value	
Model	1362.17	9	151.35	1.70	0.0501	Significant
A-Lipid	98.00	1	98.00	1.10	0.0422	
B-Surfactant	364.50	1	364.50	4.09	0.0989	
C-Co-surfactant	18.00	1	18.00	0.2022	0.6718	
AB	361.00	1	361.00	4.05	0.1002	
AC	100.00	1	100.00	1.12	0.0377	
BC	1.0000	1	1.0000	0.0112	0.0197	
A^2	77.56	1	77.56	0.8712	0.3935	
B^2	136.64	1	136.64	1.53	0.2704	
C^2	176.64	1	176.64	1.98	0.2180	
Residual	445.17	5	89.03			
Lack of Fit	140.50	3	46.83	0.3074	0.8227	not significant
Pure Error	304.67	2	152.33			
Cor Total	1807.33	14				

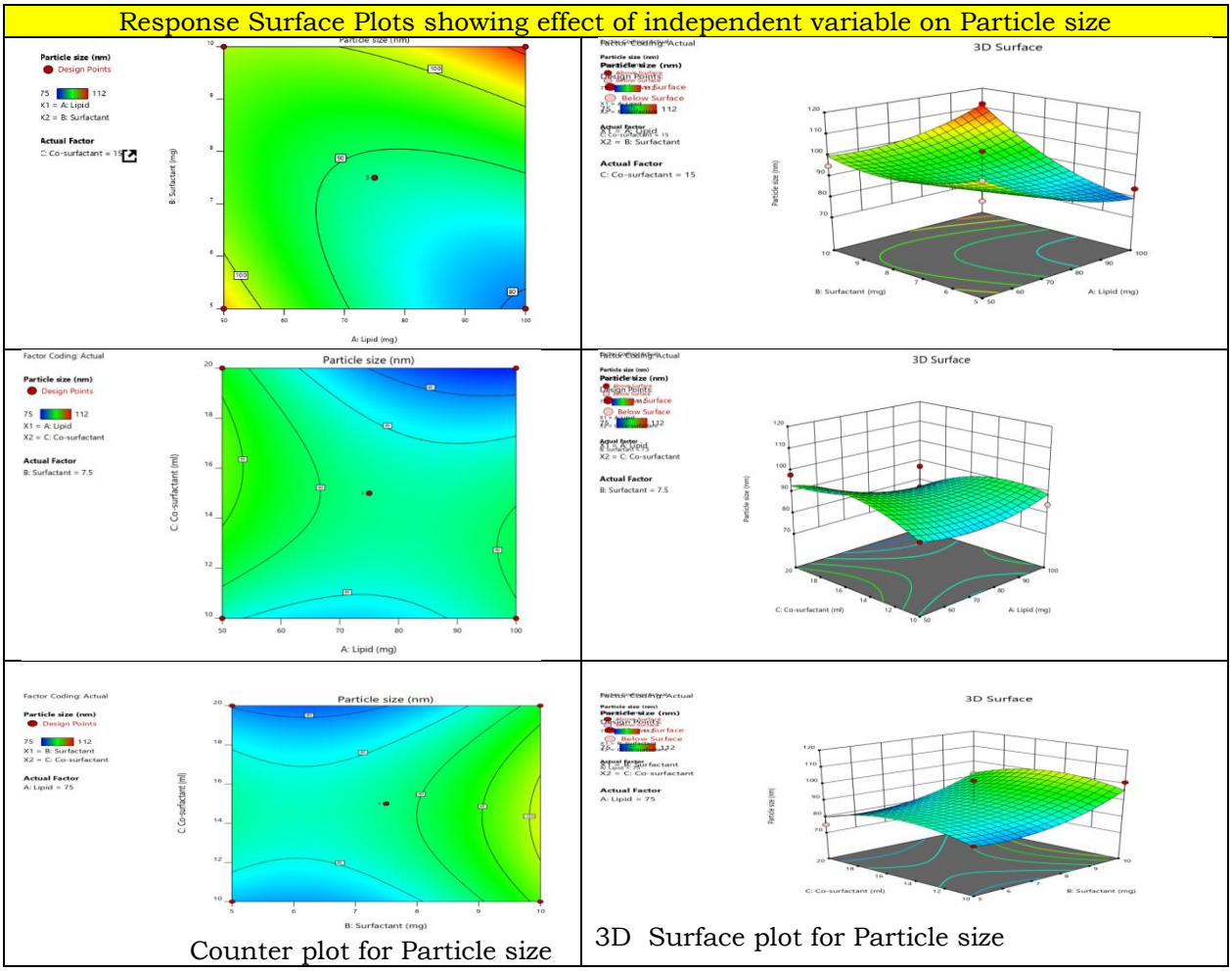

Fig 9. Response Surface Plots showing effect of independent variable on Particle size

Table 10
ANOVA Table for Entrapment Efficiency% Quadratic model

Response 2: Entrapment Efficiency

Source	Sum of Squares	df	Mean Square	F-value	p-value	
Model	148.00	9	16.44	51.18	0.04515	Significant
A-Lipid	69.03	1	69.03	4.94	0.0568	
B-Surfactant	10.49	1	10.49	0.7512	0.04257	
C-Co-surfactant	10.81	1	10.81	0.7744	0.01191	
AB	3.44	1	3.44	0.2465	0.04006	
AC	7.16	1	7.16	0.5125	0.50061	
BC	24.45	1	24.45	1.75	0.02430	

A^2	20.33	1	20.33	1.46	0.02816	
B^2	0.7686	1	0.7686	0.0551	0.0338	
C^2	1.05	1	1.05	0.0753	0.01947	
Residual	69.81	5	13.96			
Lack of Fit	9.77	3	3.26	0.1085	0.9476	not significant
Pure Error	60.04	2	30.02			
Cor Total	217.81	14				

Response Surface Plots showing effect of independent variable on Entrapment Efficiency

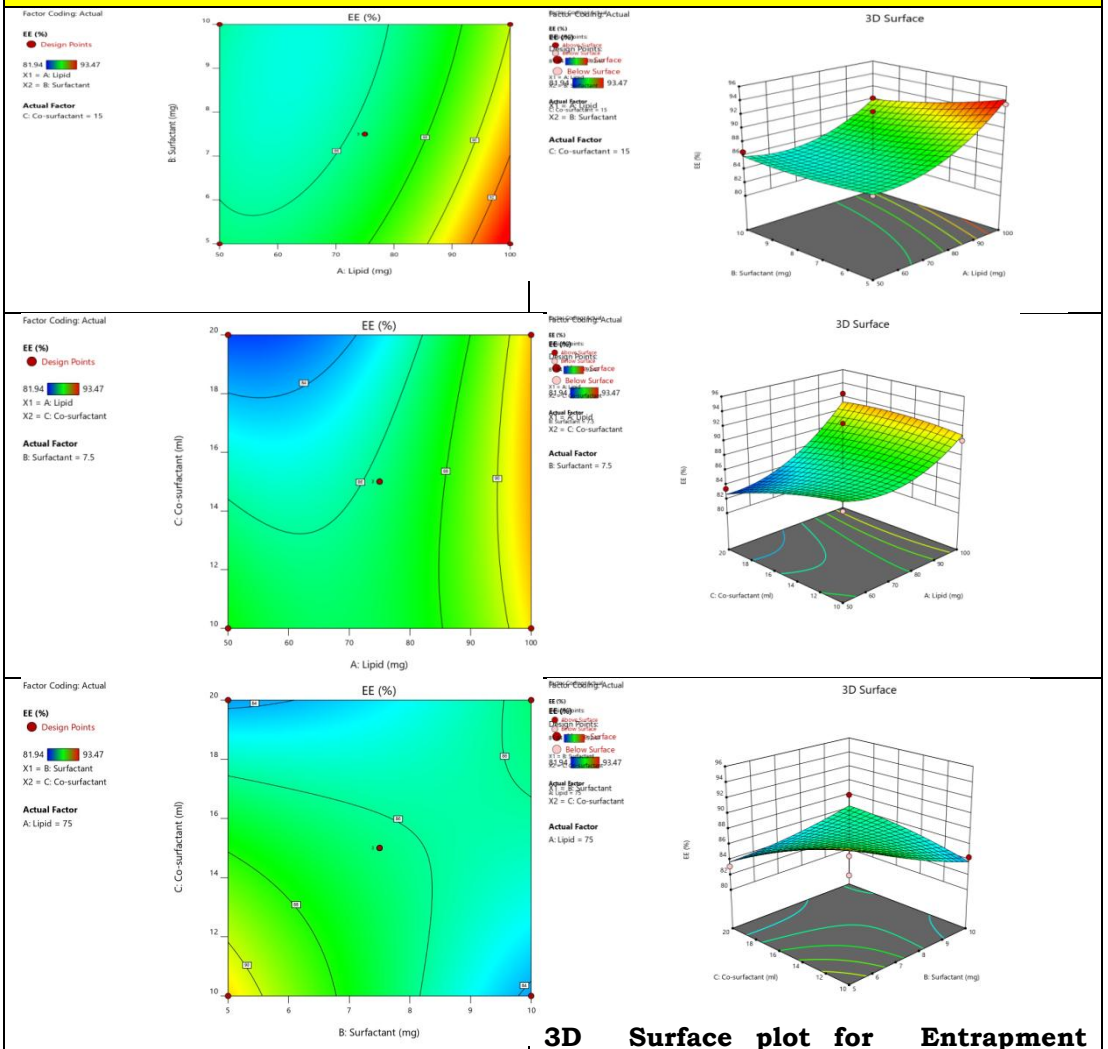

Counter plot for Entrapment Efficiency

3D Surface plot for Entrapment Efficiency

Fig 10. Response Surface Plots showing effect of independent variable on Entrapment

Table 11
ANOVA Table for Zeta Potential Quadratic model

Response 3: Zeta Potential

Source	Sum of Squares	df	Mean Square	F-value	p-value	
Model	132.03	9	14.67	42.25	0.01928	Significant
A-Lipid	3.32	1	3.32	0.5083	0.05078	
B-Surfactant	11.47	1	11.47	1.76	0.02421	
C-Co-surfactant	4.91	1	4.91	0.7534	0.04251	
AB	0.6006	1	0.6006	0.0921	0.03738	
AC	64.96	1	64.96	9.96	0.02521	
BC	7.70	1	7.70	1.18	0.02681	
A^2	0.4001	1	0.4001	0.0613	0.01432	
B^2	0.5520	1	0.5520	0.0846	0.08282	
C^2	38.98	1	38.98	5.98	0.05833	
Residual	32.61	5	6.52			
Lack of Fit	18.90	3	6.30	0.9192	0.5587	not significant
Pure Error	13.71	2	6.86			
Cor Total	164.65	14				

Response Surface Plots showing effect of independent variable on Zeta Potential

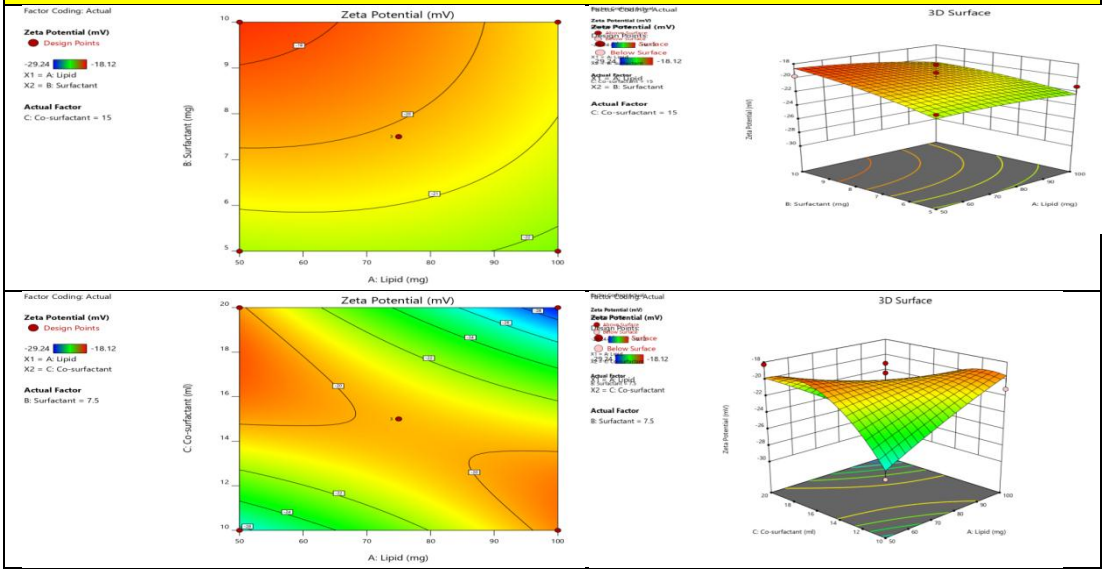

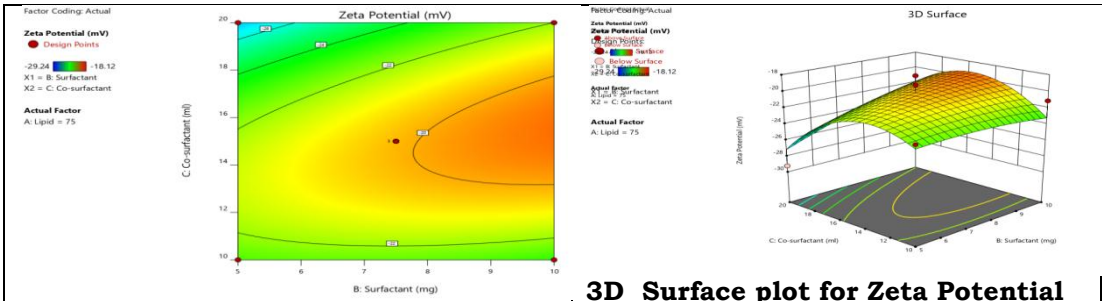

Counter plot for Zeta Potential **3D Surface plot for Zeta Potential**

Fig 11. Response Surface Plots showing effect of independent variable on Zeta Potential

Optimization

Preliminary prepared DG-NLCs were optimized by QbD software (Box-Behnken design). Data of all responses of each were fitted into various models like linear, 2nd order and quadratic. The quadratic model was found to best fit for all responses because it has a high value of regression coefficient than other. The experimental and predicted value of each response was found to very close to each other, it indicated high value of regression coefficient and well fitted and it proved by previously published research24. ANOVA of best-fitted model (quadratic) of every response(PS, EE and drug release) were calculated and expressed in Table 19-21 . P <0.0001 was found for a quadratic model of all responses indicated that model was significant. The lack of fit of model was found to be non-significant ($p>0.05$) , indicated less variation in actual and predicted value and model is well fitted as well as independent factors are extensive effect on responses. Regression value (R2) of all applied models were found to be maximum for quadratic (R2 =0.9999) . The polynomial equation as shown below, 3-D and contour plots for each response were generated and expressed in Figures 35-37. It expressed the contribution of variables over individual response. For quantitative analysis, actual vs predicted value graph of each responses were expressed by Supplementary Figure and have high value of regression coefficient (R2 =very close to one) , indicating both values not have significantly

Impact of Independent Variables on Response Particle Size (Y1)

Influences of factors i.e., lipid (A) , surfactant (B) and Co-surfactant (C) on PS (Y1) was mathematically expressed by a software-generated polynomial equation of quadratic model given bellow.

$$Y1=81.63+32.82A-82.85B-27.84C-14.48AB+2.53AC-5.82BC+1.65A^2+3.72B^2-4.28C^2$$

The positive and negative sign represents the favour and unfavoured effect on PS. In this case, A, B, C, AB, AC, BC, A2, B2, C2 are significant model terms because it has $p< 0.05$. The F-value of the model from ANOVA analysis was found to be 32325.99, revealed that the model is significant. R2 of particle size is 0.9999 for

the quadratic model and it significantly greater than other models represented that quadratic is a suggested model. The lack of fit for suggested model is nonsignificant（p＞0.05, F-value-0.12） confirm that model was well fitted into given data. The adequate precision was fond to be 658.831 indicates an adequate signal. The PS of all fifteen formulations was found in the range of 65nm-112 nm, respectively. It was found that concentration of lipid increases the PS of NLCs increase because it increases the viscosity of solution, decreases emulsifying efficiency of surfactant, increased the interfacial tension leads to particle agglomeration. This result was agreed with previously published work like optimization of lurasidone NLCs for brain delivery

Impact of independent variable over Entrapment efficiency %

Influence of lipid (A), surfactant（B）and Co-surfactant（C）over the EE（Y2）was mathematically expressed by the software-generated polynomial equation given bellow.

Y2＝＋88.29＋5.15A＋9.12B＋7.28C－1.21AB－2.45AC ＋0.32BC＋2.91A2 －7.54B2 －4.20C2

The model fisher's ratio（F）was found to be 2638.43 from ANOVA analysis, implies that model is significant. The model term i.e., A, B, C, AB, AC, BC, A2, B2 , C2 are significantly affected on the response（p＜0.05). The lack of fit was found to be nonsignificant（F＝1.68, P＝0.3081, p＞ 0.05), clearly confirm that model was well fitted into given data31). The model R2 is 0.9999（close to unity）indicated that well-fitted. The predicted R2 of 0.9972 is in reasonable agreement with the adjusted R2 of 0.9993. The adequate precision（signal to noise ratio）of model is 178.86（＞4), indicted that model was well fitted34). The% EE of drug of all seventeen formulations was found in the range of 60.43 to 96.54%.The polynomial equation showed that all independent variables showed a positive effect on EE（synergisticeffect）but interaction showed negative（AB, & AC） and positive（BC）effect on EE. Interaction effect is less prominent than the individual variable. It was observed that increased lipid concentration, the EE increases because of more space available for housing as well as minimized escaping of drug to external phase. This result agreed to previously published work i.e., optimization of oral NLCs delivery of isradipine

Impact of Independent Factor on Zeta Potential

Influences of lipid （A）, surfactant（B）and Co-surfactant（C）on zeta potential（Y3）was mathematically expressed by a software-generated polynomial equation of quadratic model given bellow.

Y3＝＋78.58－4.16A＋4.63B＋3.11C＋2.23A B－2.29AC －0.90BC－3.79A2 －0.51*B2 －1.39*C2

Desirability

Desirability, Particle size, %EE and Zeta potential of Surfactant vs Lipid are shown in Figure 12.

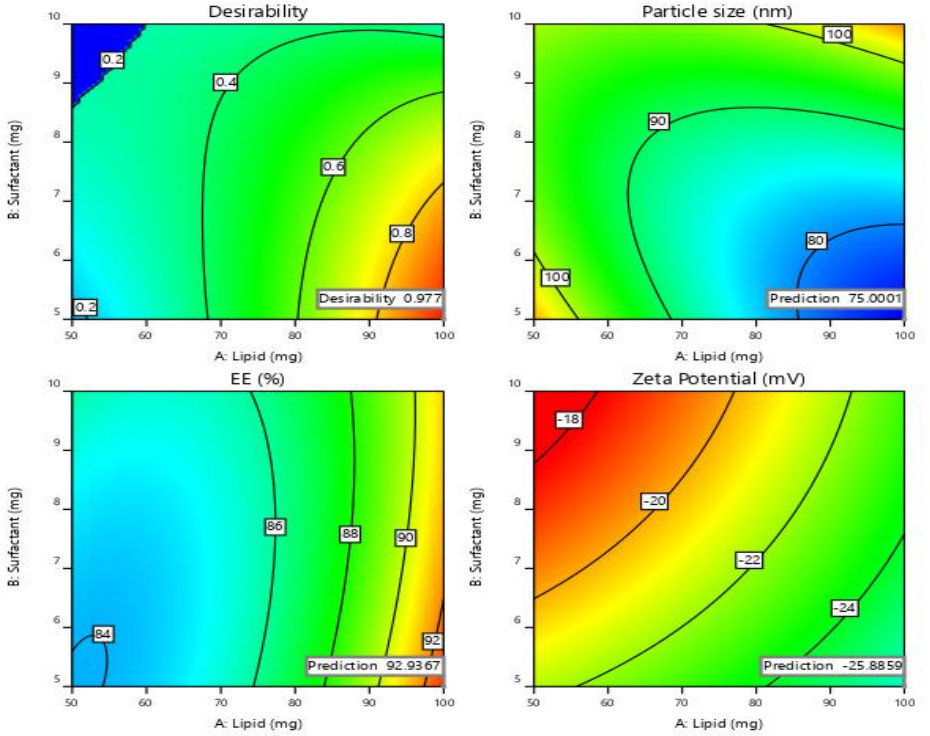

Fig 12. Desirability, Particle size, %EE and Zeta potential of Surfactant vs Lipid

Scanning Electron Microscopy

SEM photomicrograph of OPT-DPLNC is shown in Figure 13. The nonporous, spherical particles with a smooth surface were observed for the lyophilized NLC-C2. These observed particle diameters were found to be slightly greater than the diameters of DLS. The increase in diameter might be due to lyophilisation of NLC formulation.

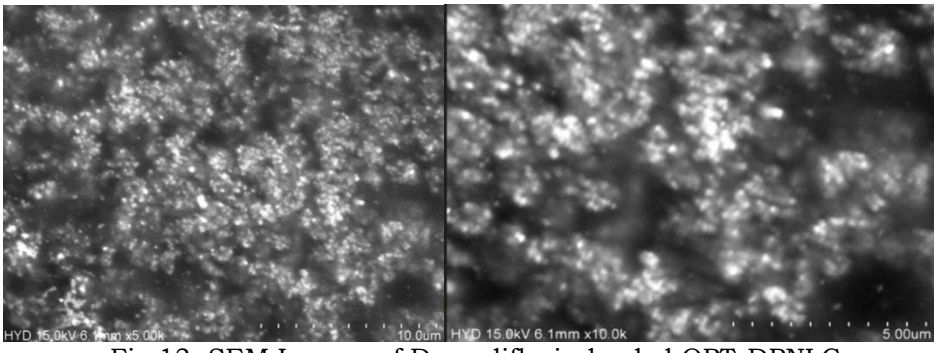

Fig 13. SEM Images of Dapagliflozin loaded OPT-DPNLC

***Ex-vivo* Permeation Study**

Figure 14 showed ex vivo permeability of OPT-DPNLC and DP-dispersion in intestinal sac. OPT-DPNLC exhibited significantly ($p<0.05$) high permeation (290 µg/cm) than DP-dispersion (70µg/cm) . Flux was measured from slop of amount of drug permeated vs. time. OPT-DPNLC (1.293 µg/cm2 /h) have 4.8-fold higher flux than DP-dispersion (0.2683 µg/cm2 /h. Table 12 shows permeation parameters of pure drug and OPT-DPNLC formulation across rat intestine.

Table 12
Permeation Parameters of Pure drug and OPT-DPNLC formulation across rat intestine

Formulation	Intial concentration in donar compartment(µg)	Area (cm^2)	Slope	Q2h(µg)	Jss(µg/cm^2/h)	Kp(cm/h)x 10^{-8}	ER	Intial concentration in donar compartment(µg)
Pure drug	5000	22.4	0.001	1950	0.00004464	0.892857	--	5000
OPT-DPNLC	5000	30.4	0.005	4000	0.00016447	3.289470	3.68	5000

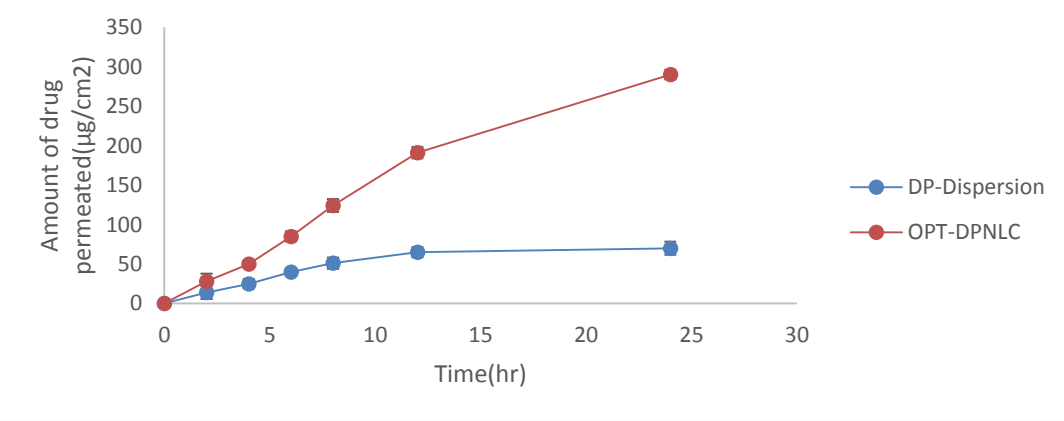

Fig 14. Ex-vivo permeation study parameters

The APC for **OPT-DPNLC** and DP-dispersion was found to be 4.14×10−5 and 8.61×10−6 cm/min respectively. The high permeation of NLCs is due to colloidal size, which increases surface area and more energy contact between DG, lipid and surfactant as well as due to permeation enhancing capacity lipid and surfactant. It changing tight junction opening of intestinal sac due to high hydrostatic pressure and possess of drug through Para cellular transport. Also, surfactant diminished intestinal efflux of the formulation by inhibiting Pgp efflux pump of enterocytes as well as reducing uptake of the reticuloendothelial system

Conclusion

The chosen experimental design for response surface methodology, i.e., Box-Bhenken design, mathematical model for generation of i.e., multiple linear regression analysis, and the methods for location of optima i.e., overlay plots and desirability function, all successfully vouched the appropriate selection of the optimized formulation, Optimized formulation was prepared and found to be PS of 69.99 nm, EE of 81.94% and Zeta potential -28.99 respectively. The predicted value of optimized formulation from software was PS of 70.22 nm, EE of 81.72% and zeta potential -29.24 The OPT-DP-NLC formulations showed 100.11%, 100.26 % and 100.13% of prediction of predicted value of responses (Y1, Y2, & Y3. Ex-vivo permeation for Optimized Dapagliflozin loaded NLC was performed in intestinal segment of rats. The APC for OPT-DPNLC and DP-dispersion was found to be $4.14\times10-5$ and $8.61\times10-6$ cm/min respectively. The high permeation of NLCs is due to colloidal size, which increases surface area and more energy contact between DG, lipid and surfactant as well as due to permeation enhancing capacity lipid and surfactant.

References

1. Gadadare, R., Mandpe, L., Pokharka, V., 2015. Ultra rapidly dissolving repaglinide nanosized crystals prepared via bottom-up and top-down approach: influence of food on pharmacokinetics behavior. AAPS PharmSciTech.16(4), 787-799.
2. Veiseh, O., Tang, B.C., Whitehead, K.A., Anderson, D.G., Langer, R., 2015. Managing diabetes with nanomedicine: Challenges and opportunities. Nat Rev Drug Discov. 14, 45-57.
3. Matthaei, S., Stumvol,l M., Kellere,r M., Haring, H.U., 2000. Pathophysiology and pharmacological treatment of insulin resistance. Endocr Rev. 21, 585–618.
4. Nimase, P.K., Vidyasaga,r G., Suryawanshi, D.M., Bathe, R.S.,2013. Nanotechnology and diabetes. Int J Adv Pharmaceutics. 2, 145-148.
5. Zanchetta, B., Chaud, M., Santana, M., 2015. Self-emulsifying drug delivery systems (SEDDS) in pharmaceutical development. J. Adv. Chem. Eng. 5, 1–7, 2015.
6. Aslam, M., Aqi,l M., Ahad, A., Najmi, A.K., Sultana, Y., Ali, A.,2016. Application of Box–Behnken design for preparation of glibenclamide loaded lipid based nanoparticles: Optimization, in vitro skin permeation, drug release and in vivo pharmacokinetic study. *Journal of Molecular Liquids. 219*, 897-908.
7. Alam, S., Aslam, M., Khan, A., 2016. Nanostructured lipid carriers of pioglitazone for transdermal application: from experimental design to bioactivity detail. Drug Deliv. 23(2), 601-609.
8. Chen, H., Zhong, Q., 2014. Processes improving the dispersibility of spray-dried zein nanoparticles using sodium caseinate. Food Hydrocolloids. 35, 358–366.
9. Teixeira, J., 1998. Small-angle scattering by fractal systems. J. Appl. Crystallogr. 21 (6), 781–785.

10. Maringanti, P.S., Nalagonda, C., 2013. Formulation and evaluation of sitagliptin phosphate and metformin hydrochloride trilayered tablets. Int J Drug Deliv. 5, 15.
11. Kasim, N.A., Whitehouse, M., Ramachandran, C., Bermejo, M., Lennernäs, H., Hussain, A.S, Junginger, E., Stavchansky, S.A., Midha, K.K., Shah, V.P., Amidon, G.L.,2004. Molecular properties of WHO essential drugs and provisional biopharmaceutical classification. Mol. Pharm. 1 (1), 85–96.
12. Ahmadi, A., Khalili, M., Farsadrooh, M., Ghiasi, M., Nahri-Niknafs, B.,2013. Antihyperglycemic and antihyperlipidemic effects of newly synthesized glibenclamide analogues on streptozotocin-diabetic rats. Drug Res. 63 (12).
13. Arya, A.K., Kumar, L., Pokharia, D., Tripathi, K., 2008. Applications of nanotechnology in diabetes. Dig J NanomaterBiostruct. 3, 221-225.
14. Sharma, G., Sharma, A.R., Nam, J.S., Doss, G.P.C., Lee, S.S., 2015. Nanoparticle based insulin delivery system: The next generation efficient therapy for Type 1 diabetes. Nanobiotechnol.13, 74.
15. Mudshinge, S.R., Deore, A.B., Patil, S., Bhalgat, C.M., 2011. Nanoparticles: Emerging carriers for drug delivery. Saudi Pharm J.19(3), 129-141.
16. Hasan, A.A., Madkor, H., Wageh, S., 2013. Formulation and evaluation of metformin hydrochloride-loaded niosomes as controlled release drug delivery system. Drug Deliv. 20(3-4), 120-126.
17. Elbahwy, I.A., Ibrahim, H.M, Ismael, H.R., Kasem, A.A., 2017. Enhancing bioavailability and controlling the release of glibenclamide from optimized solid lipid nanoparticles. J. Drug Delivery Sci. Technol. 38, 78–89.
18. Herman, G.A., Bergman, A., Liu, F., 2006. Pharmacokinetics and pharmacodynamic effects of the oral DPP-4 inhibitor sitagliptin in middle-aged obese subjects. J Clin Pharmacol. 46, 876–886.
19. Tamjidi, F., Shahedi, M., Varshosaz, J., Nasirpour, A., 2013. Nanostructured lipid carriers (NLC): A potential delivery system for bioactive food molecules. Innov. Food Sci. Emerg. Technol.2013:19, 29–43.